Catalysis Today 156 (2010) 237–245

Contents lists available at ScienceDirect

Catalysis Today

journal homepage: www.elsevier.com/locate/cattod

The oxidative dehydrogenation of *n*-butane in a differential side-stream catalytic membrane reactor

David Milne*, Tumisang Seodigeng, David Glasser, Diane Hildebrandt, Brendon Hausberger

Centre of Material and Process Synthesis, University of the Witwatersrand, Johannesburg, Private Bag 3, WITS 2050, South Africa

ARTICLE INFO

Article history:
Available online 27 April 2010

Keywords:
Attainable region
Recursive Convex Control Policy Algorithm
Butane
Oxidative dehydrogenation
Differential side-stream reactor

ABSTRACT

The synthesis of butenes and butadiene from the oxidative dehydrogenation of *n*-butane is a chemical reaction of economic relevance and the choice of catalyst is of considerable importance. In this simulation exercise a V/MgO catalyst in a differential side-stream catalytic membrane reactor was studied.

The Recursive Convex Control (RCC) algorithm was used to determine the operating parameters required to determine the maximum yields of hydrocarbon products. The algorithm, in addition to selecting for the duty a single differential side-stream catalytic membrane reactor (DSR) in preference to a CSTR and a PFR, also developed the profile for the optimal addition of oxygen along the length of the reactor.

The maximum yield of butenes, all three isomers, was found to be 0.119 carbon mass fraction.

The maximum yield of butadiene from the ODH of *n*-butane was found to be 0.799 carbon mass fraction.

The rates of formation of hydrocarbon reactants and products are discussed.

Statistical analyses of the ratios of formation rates of the butene isomers and of carbon dioxide to carbon monoxide are presented.

The interplay between alternative reaction routes for the formation of butadiene is reviewed as well as the validity of the kinetic data at low oxygen partial pressures.

1. Introduction

The attainable region (AR) method uses geometrical principles to determine the multi-dimensional spatial region in which all the reactants and products for reaction systems with known kinetics can be found. The AR method can also be used to find the maximum yield of product as well as the reactor types and configurations necessary to yield any slate of products within this spatial region. It has been shown by Feinberg and Hildebrandt [1] that only three basic reactor types, a continuously stirred tank reactor (CSTR), a plug-flow reactor (PFR) and a differential side-stream reactor (DSR), in suitable configurations, are sufficient to provide any yield of reaction products. In the absence of a complete sufficiency condition, a presumed AR is usually termed a candidate AR (AR^C).

It is not the intention in this paper to describe AR theory in detail. Instead, the attention of the reader is directed to the work of Glasser et al. [2,3] and Feinberg [4,5] for a comprehensive review of Attainable Region theory and practice.

Recently the Recursive Convex Control (RCC) algorithm has been developed and used successfully to analyse complex chemical reactions. These reactions, by virtue of many possible products, can be considered as possessing many dimensions to which can be added the further dimension of residence time. The RCC algorithm has been proved to be capable of solving multi-dimensional problems of a complexity previously considered too difficult to handle. Again, the characteristics of the RCC and its usage shall not be discussed in detail in this paper. Rather the attention of the reader is directed to the work of Seodigeng [6,7] for an extensive description of its capabilities. Suffice it to say that the use of the RCC algorithm requires no prior understanding of AR theory to use it successfully. However, knowledge of AR principles is useful in analysing the outputs from the RCC method. Another feature of the RCC algorithm is that no prior reactor assumptions are necessary as the recommended reactor type(s) and their sequencing are determined by the algorithm.

N-butane and oxygen are supplied together at the tube inlet of a shell and tube reactor at atmospheric pressure and at a temperature of 773K. The reactor tubes are packed with a V/MgO catalyst containing 24 wt% of V_2O_5. A side-stream of oxygen at a pressure of up to 6 atm inside the shell diffuses through the inert porous inorganic membrane tube wall to react with the hydrocarbons inside the tubes which are packed with the catalyst. Téllez et al. [8,9] used a SiO_2-modified α-Al_2O_3 membrane tube wall to distribute oxygen to the V/MgO catalyst inside the tubes. The pressure inside the tubes was taken to be 1 atm. The partial pressure of oxygen to the reactor

Abbreviations: AR, attainable region; AR^C, candidate attainable region; CSTR, continuously stirred tank reactor; DSR, differential side-stream catalytic membrane reactor; IMR, inert membrane reactor; ODH, oxidative dehydrogenation; PFR, plug flow reactor; RCC, Recursive Convex Control algorithm.

* Corresponding author at: 16 Rooibos Avenue, Allen Grove, Kempton Park 1619, South Africa. Tel.: +27 11 394 7683; fax: +27 11 717 7557.
E-mail address: admilne@mweb.co.za (D. Milne).

0920-5861/$ – see front matter © 2010 Elsevier B.V. All rights reserved.
doi:10.1016/j.cattod.2010.03.033

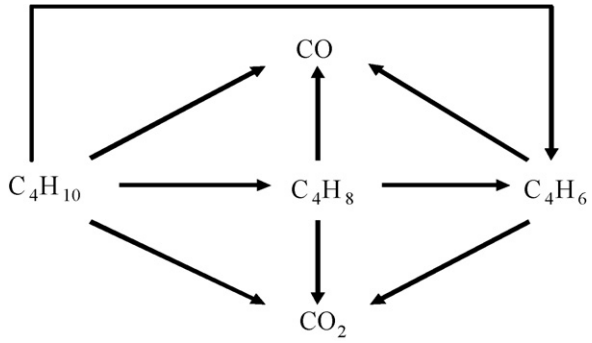

Fig. 1. Reaction network for the oxidative dehydrogenation (ODH) of *n*-butane to butenes and butadiene.

was used as the primary control variable. The reaction network for the ODH of n-butane [8,9] is shown in Fig. 1.

This reaction network clearly shows the complexity of the ODH process. Omitted from the scheme is the formation of water which is present *ab initio*. Of particular interest are the two reaction routes for the oxidation of *n*-butane to butadiene, one direct and the other through the synthesis of butenes and their subsequent oxidation to butadiene. We shall discuss this later in the paper.

The kinetic data for the system, rates of formation, kinetic equations and data for the ODH of *n*-butane, 1-butene and butadiene are shown in Appendix A.

2. Experimental

Our previous papers [10,11] showed that the maximum possible theoretical yields of butenes and butadiene from the ODH of *n*-butane could be derived from an inert membrane reactor (IMR) where the oxygen partial pressure was maintained at a very low and constant value along the length of the reactor. In line with Attainable Region terminology we shall refer henceforth to this IMR as a DSR. Whereas the ensuing IMR, i.e. DSR, was of an impractical size what did emerge from these studies were the theoretical maximum yields of hydrocarbon products possible from the ODH process. This then presented the challenge of determining the necessary process conditions to achieve these maxima in a smaller reactor. Again, in our earlier papers, we began with considering only a DSR and neglected the possibility that a PFR (or even a CSTR), in some configuration with a DSR, might prove to be a better option. That the optimal reactor configuration, without having to make any prior assumptions regarding reactor types, emerges from the analysis of the RCC results is one of the strengths of this tool.

With the reaction scheme in Fig. 1 there is a very large increase in the number of moles as the reaction proceeds. To use the AR method with linear mixing laws, all hydrocarbon concentrations are expressed in terms of mass fractions of carbon, the number of carbon atoms remaining constant from the beginning to the end of the reaction.

In the ODH of *n*-butane, the reaction system comprises nine chemical species including oxygen and water. When residence time is considered, the ODH of *n*-butane requires a 10-dimensional space for a complete description. In our earlier papers [10,11] the kinetic equations were applied to the nine species within the 10-dimensions from which two-dimensional projections were abstracted. Where extensions of these two-dimensional concentration spaces were possible, i.e. through the elimination of any concave areas, they were done solely within the two-dimensional spaces and not by intrusion into higher dimensional hyperspaces.

In an attempt to keep the paper as focussed as possible on the results from the RCC tool, we have assumed an isothermal condition of 773 K and a constant tube pressure of 1 atm. These assumptions also were applicable to our earlier papers [10,11] and the relevance of the results from the RCC tool to those from the earlier papers depended upon identical operating parameters. Non-isothermal heat transfer in the determination of attainable regions has been investigated in particular by Hildebrandt et al. [12], Nicol et al. [13] and Godorr et al. [14].

In a recent paper, Milne et al. [15] have described in greater detail the application of the RCC method to the ODH of *n*-butane and 1-butene.

3. Results

The RCC algorithm has been employed to identify candidate attainable regions (AR^Cs) and yields of hydrocarbon products for the following reactions.

- Case 1: ODH of *n*-butane to form butenes (all three isomers).
- Case 2: ODH of *n*-butane to form butadiene.

The partial pressure of oxygen in the feed was varied between 85 kPa and a very low value and should a DSR be selected by the RCC algorithm as one of the three possible reactors additional oxygen would be supplied *optimally* along the length of the DSR so as to attain the profile of the AR^C. This reactor configuration is styled a *critical* DSR [1,16].

The results of these calculations are values of concentrations in terms of carbon mass fractions of the boundary values of a convex region in a higher dimensional space. In order to present these results in a way that is understandable to the reader we will present graphical results of two-dimensional projections in terms of the variables of interest.

3.1. Case 1—ODH of n-butane to form butenes

In the ODH of *n*-butane to butenes, we have nine possible chemical substances. These include oxygen and water as well as the oxidation both of butane and butenes to butadiene, the latter in this case being considered as an undesirable by-product. To these nine substances, a tenth variable, residence time, can be added.

Our earlier paper [11] found that a butenes yield of 0.119 carbon mass fraction was the theoretical maximum yield possible from the ODH of *n*-butane.

Fig. 2 is the two-dimensional projection of the AR^C identified by the RCC method for the ODH of *n*-butane to butenes.

Fig. 2 shows the extreme points of the profiles in mass fraction space for the yield of butenes (sum of all three isomers) from the ODH of *n*-butane as derived from the application of the RCC algo-

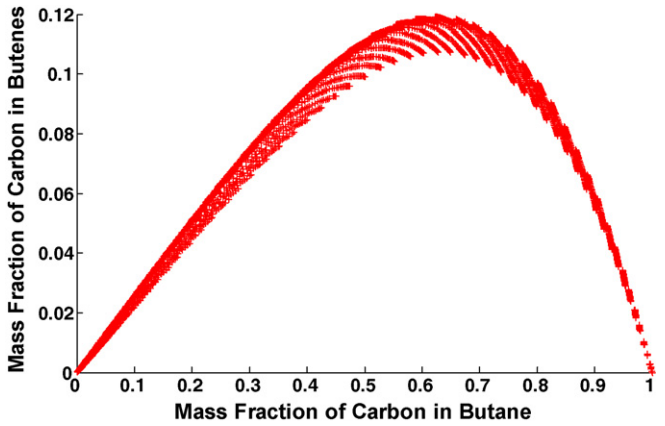

Fig. 2. Projection of the set of extreme points derived from the RCC profile for the ODH of *n*-butane to butenes (sum of all three isomers) plotted in mass fraction space.

rithm. Fig. 2 is a two-dimensional projection from a 10-dimensional hypersurface.

In our earlier paper [11], the outer bound of the profile shown in Fig. 2 was associated with an extremely low and constant value of oxygen partial pressure. A very large and impractical residence time also was required. The RCC method, as shall be shown later in this paper, attained the profile shown in Fig. 2 by judiciously controlling the addition of the oxygen in the DSR resulting in a significantly lower residence time.

The lower bound of the RCC profile in Fig. 2 corresponds to an initial oxygen partial pressure of 85 kPa and the upper bound to a low partial pressure value. Our previous paper [11] showed that the upper bounds of this region for constant oxygen partial pressures of 0.25 kPa and an extremely low value were indistinguishable so close were they together.

Fig. 2 shows that at a low value of oxygen partial pressure the maximum yield of butenes (the sum of all three isomers, 1-butene, trans-2-butene and cis-2-butene) from the ODH of *n*-butane is 0.119 carbon mass fraction and occurs at a *n*-butane concentration of 0.623. The maximum yield from the lower bound is 0.103 carbon mass fraction. We conclude that the maximum yields of butenes are relatively insensitive to the partial pressure of oxygen. Despite the reduction of this partial pressure from 85 kPa to a low value, the maximum yield of butenes increased by less than 16%. Our earlier paper [11] commented that the selectivity of butane for the maximum yield of butenes is but slightly influenced by the oxygen partial pressure.

Detailed analysis of the results from this RCC application (to be shown later in this paper) confirmed that the outermost limit was commensurate with a DSR to which the supply of oxygen was controlled according to a specific regimen (not necessarily a constant value of 0.25 kPa.)

Fig. 3 is a breakdown of the upper bound of Fig. 2 to show the isomeric constituents and their contribution to the outer bound's values. A characteristic of Fig. 3 is the preferential synthesis of 1-butene followed by cis-2-butene with trans-2-butene having the lowest rate of formation. In the absence of kinetic data for the ODH of the individual isomers to carbon monoxide, carbon dioxide, water and butadiene, we cannot exclude the possibility that the reaction rate for the subsequent ODH of trans-2-butene exceeds that for cis-2-butene and the latter, in turn, is greater than that for 1-butene.

The maximum yields of the individual isomers at the low oxygen partial pressure mandated by the RCC method are 0.055, 0.035 and 0.029 carbon mass fractions respectively for 1-butene, cis-2-butene and trans-2-butene and are associated with a butane concentration of 0.623 carbon mass fraction.

The selectivity of butane to butenes at any point of the profile in Fig. 2 is given by the ratio of its *y*-coordinate to the distance of its horizontal projection on the *x*-axis from the feed point. Another way of saying this is that the selectivity at any point of the profile is equal to the tangent of the angle between the *x*-axis and a line from the feed point to the relevant point on the profile. It is clear from Fig. 2 that the maximum selectivity occurs at the feed point and thereafter diminishes. It retains a positive value until the maximum point of the profile is attained and then becomes negative. The butane-butenes profile is convex over its entire perimeter and a property of a convex profile is the occurrence of maximum selectivity at the feed point.

The ratio of the yields of the three isomers, relative to trans-2-butene, was found to be constant over the spectrum of oxygen partial pressures. The ratios of formation were found to be 1.9:1.2:1 for 1-butene:cis-2-butene:trans-2-butene and are shown in Fig. 4. This is only to be expected. Referring to Table 2 in Appendix A at the end of this paper, the rate expressions for the oxidation of n-butane to the three isomers of butene, $r1$, $r2$ and $r3$, are functions of the partial pressure of *n*-butane and the selective oxidation of the catalyst sites, θ_0. What differentiates these rate expressions are the respective rate constants, $k1$, $k2$ and $k3$ (Table 3) and the ratios of these rate constants for 1-butene, cis-2-butene and trans-2-butene are 1.9, 1.2 and 1.0 respectively.

In Fig. 5 we show the optimal control policy derived from the RCC algorithm for the distribution of oxygen along the length of the

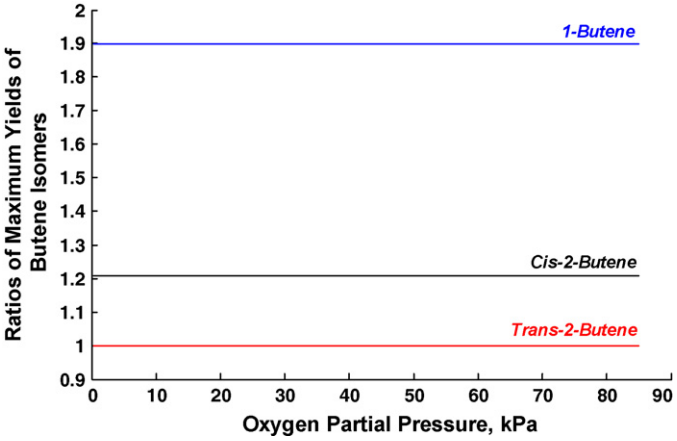

Fig. 4. Ratio of yields of butene isomers relative to trans-2-butene as functions of oxygen partial pressre.

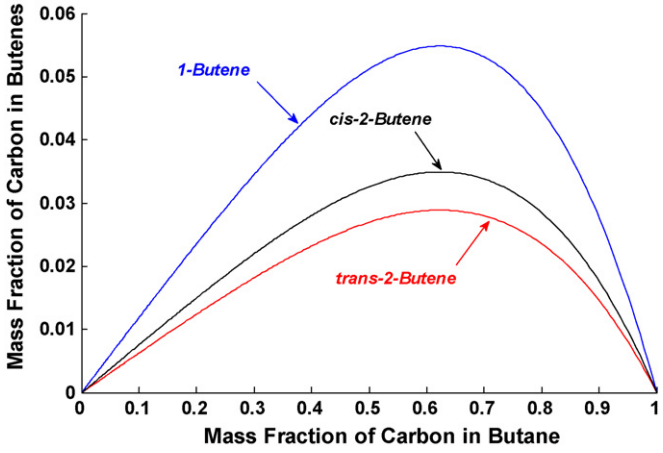

Fig. 3. Breakdown of Fig. 2 to show the individual profiles of the three butene isomers plotted in mass fraction space at a very low value of oxygen partial pressure.

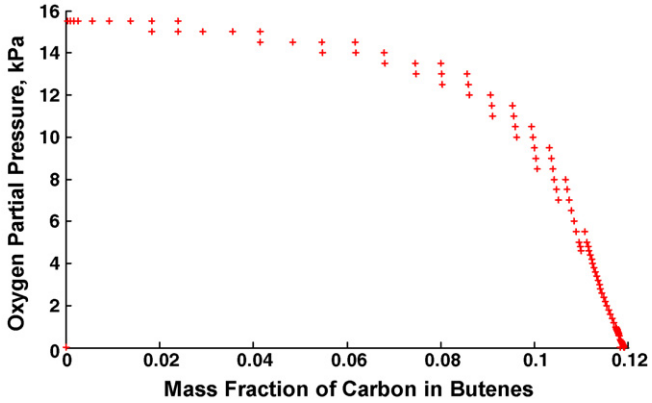

Fig. 5. RCC operational oxygen control policy for the maximum yield of butenes from the ODH of *n*-butane.

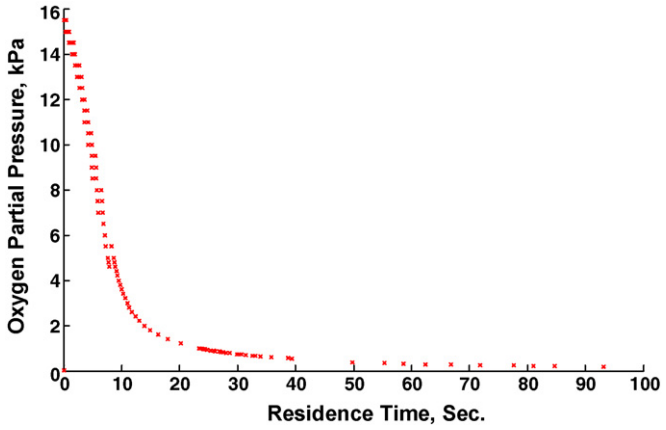

Fig. 6. RCC oxygen control policy as a function of residence time for the maximum yield of butenes from the ODH of *n*-butane.

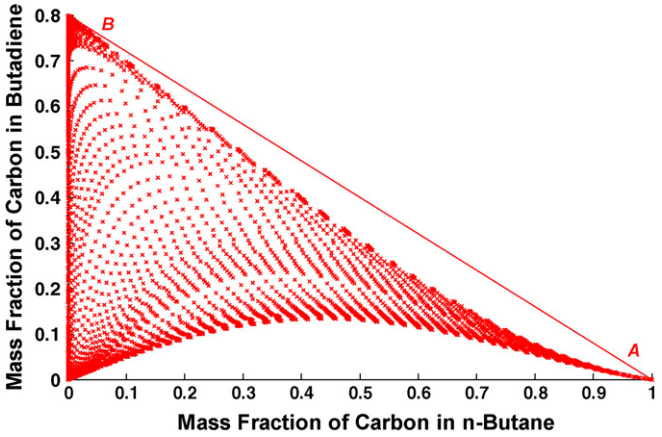

Fig. 7. Set of extreme points derived from the RCC profile for the ODH of *n*-butane to butadiene in mass fraction space.

reactor as a function of the yield of butenes. Fig. 5, in effect, says that the initial partial pressure to the reactor should be 15.5 kPa and should be held constant at this level by the addition of fresh oxygen until the yield of butenes has reached 0.025 carbon mass fraction. This implies that initially the reactor should be a DSR with a policy of constant oxygen partial pressure.

Once the yield of butenes has attained 0.025 carbon mass fraction, there is a change in the oxygen partial pressure. It now starts to wane from a value of 15.5 kPa to a low value. According to the RCC results, if the oxygen partial pressure along the remaining length of the DSR is controlled in this manner and allowed to be reduced to a low value, the maximum yield of butenes can be secured. Fig. 5 also shows that the maximum yield of butenes from the ODH of *n*-butane is relatively insensitive to oxygen partial pressures less than 2 kPa.

Fig. 6 shows the calculated optimal control policy for the addition of oxygen to the reactor as a function of residence time.

Fig. 6 shows that the partial pressure of oxygen is held constant at 15.5 kPa for approximately 0.5 s after which the oxygen is effectively allowed to be depleted at the *controlled* rate specified in Fig. 6. The total residence time for this critical DSR is approximately 100 s. The RCC results [15], Figs. 5 and 6 also showed that one can achieve virtually this maximum yield after 14 s when the oxygen partial pressure has dropped to 2 kPa. This is because of the asymptotic nature of the residence time profile close to this maximum value of butenes.

Fig. 5 should be studied in conjunction with Fig. 6.

Figs. 5 and 6 together show the operational control policy for the supply of oxygen along the length of the reactor for maximising the yield of the desired hydrocarbon product, butenes, from the ODH of *n*-butane.

Our use of the word *control* implies optimal control of the thermodynamic conditions, pressure, temperature, flow etc. for the best reaction rates and yields of hydrocarbon product. It does not refer to process control where the instrumentation is designed by suitable feed-back loops to regulate these thermodynamic conditions and to correct any deviation from the set conditions.

It is concluded that a DSR, the feed to which is a stream of *n*-butane and oxygen, the partial pressure of the latter being 15.5 kPa, is capable of providing the maximum possible yield of butenes after a total residence time of 100 s provided the supply of oxygen along the length of the DSR follows a defined pattern.

However, it must be stated that our previous papers [11,15] showed that with a residence time of 75 s, it was possible to achieve a yield of butenes of 99.7% of the theoretical maximum possible. The reactor configuration for this was a DSR with a constant oxygen partial pressure of 0.25 kPa. If the reaction were truncated once the oxygen partial pressure had dropped to 2 kPa, i.e. after 14 s, the yield of butenes would be 0.116 carbon mass fraction or 97% of the theoretical maximum.

We conclude that the controlled addition of oxygen to a DSR as shown in Figs. 5 and 6 effectively yields the theoretical maximum amount of butenes from the ODH of *n*-butane and can do so with the total depletion of the oxygen and within a residence time of 100 s. Alternatively, the RCC concept has confirmed that for a residence time of 14 s, a carefully controlled oxygen addition policy and a final oxygen partial pressure of 2 kPa it is possible to produce yields of butenes very close to the theoretical maximum quantity.

3.2. Case 2—ODH of n-butane to form butadiene

In our earlier paper [11] the theoretical maximum yield of butadiene from the ODH of *n*-butane was found to be 0.800 carbon mass fraction. All the initial feed of *n*-butane was effectively oxidised to produce this quantity of butadiene.

Fig. 7 shows the RCC profiles in mass fraction space for the yield of butadiene from the ODH of *n*-butane. It is a two-dimensional projection from a ten-dimensional hypersurface. As in Case 1 for the production of butenes from *n*-butane, in developing these profiles the RCC method considered all possible permutations and combinations of a CSTR, a PFR and a DSR to extend the profile to its furthest extreme. A single membrane DSR was identified as the reactor type required to develop the AR^C shown in Fig. 7.

The RCC maximum yield of butadiene, 0.799 carbon mass fraction, was obtained when the initial *n*-butane effectively had been totally oxidised. These concentrations agree with those shown earlier [11].

In our earlier paper [11], the outer bound of the profile shown in Fig. 7 was associated with an extremely low and constant value of oxygen partial pressure. A very large and impractical residence time also was required. The RCC method, as shall be shown later, attained the profile shown in Fig. 7 by judiciously controlling the addition of oxygen to a DSR and with a significantly lower residence time.

As discussed earlier in this paper the AR^C is the convex hull of the extreme points. Thus, the marked concavity apparent in Fig. 7 indicates a hyper-plane covering a large region of space. It was removed by mixing fresh feed, Point A, with product from Point B in various ratios, the locus for all the resulting outputs lying along the line AB. The AR^C for the system *n*-butane and butadiene was bounded by the two axes and the line AB. This region matched that identified in our earlier paper [11].

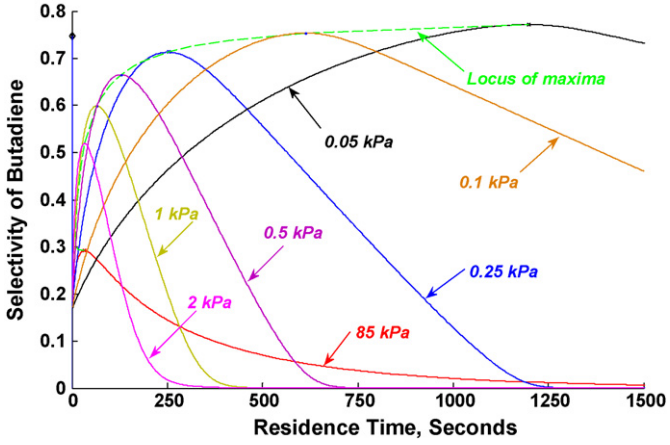

Fig. 8. Profiles of maximum selectivity of butane to butadiene at oxygen partial pressures between 0.05 kPa and 85 kPa.

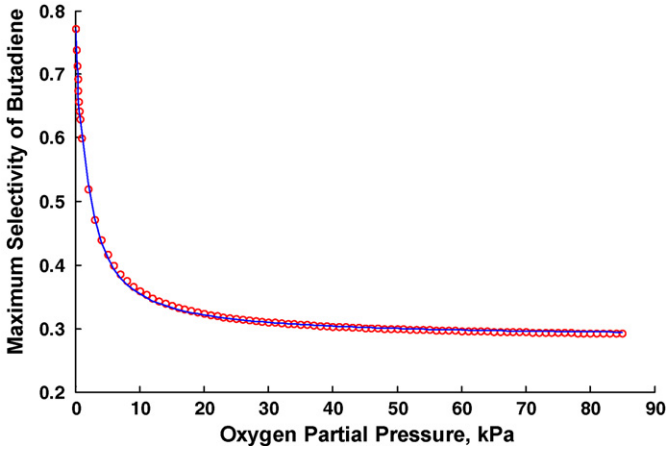

Fig. 9. Profile of maximum selectivity of butane to butadiene at oxygen partial pressures from 0.05 kPa to 85 kPa.

The butane:butadiene mass fraction profile is concave from the feed point, A, to a point B between the feed point and the zenith of the profile. At high values of oxygen partial pressure, point B lies close to point A but with the reduction in oxygen partial pressure, point B moves along the profile in the direction of the maximum. It is a property of a concave profile that the point of maximum selectivity is coincident with point B. As discussed in Case 1, the maximum value of the selectivity occurs when the tangent at a point on the profile emanates from the feed point. That this is so was shown in our earlier paper [17].

Fig. 8 below is a detailed analysis of Fig. 7 and shows the relationship between the maximum selectivity of butane to butadiene, i.e. the tangent point, at several values of oxygen partial pressure.

In Table 1 we show the residence times and butane concentrations for the values of oxygen partial pressure identified in Fig. 8.

Also shown in Fig. 8 is the locus of selectivity maxima. Initially, as the partial pressure of oxygen is reduced, the maximum selectivity of butane to butadiene increases rapidly with respect to residence time. Below 0.25 kPa, this rate of increase slows and in the limit approaches a value of 0.8 with a corresponding increase in the residence time necessary to attain this value.

Fig. 9 shows the relationship between the maximum selectivity of *n*-butane to butadiene and the oxygen partial pressure in a differential side-stream membrane reactor.

At low values of oxygen partial pressure, the profile assumes an asymptotic characteristic and as the partial pressure tends to a very low value the maximum selectivity tends to a value of 0.8. That this is so can be seen from a scrutiny of Fig. 7.

A sixth-order polynomial curve (solid line) was found to give the best fit to the calculated data (shown as circles).

The equation of this profile is

$$Y = 0.2854 + 0.7503X^{-1} - 0.6488X^{-2} + 0.2786X^{-3} - 0.0576X^{-4} + 0.0052X^{-5} - 0.0001X^{-6}$$

where Y = maximum selectivity of butane to butadiene and X = oxygen partial pressure (kPa).

This equation is valid over the range of oxygen partial pressures from 0.05 kPa to 85 kPa.

The RCC algorithm specified a total residence time of approximately 15 000 s to yield a butadiene concentration of 0.8 carbon mass fraction.

In our previous paper [11] we showed that a butadiene yield of 0.665 carbon mass fraction or 83% of the theoretical maximum could be obtained from a DSR with a constant oxygen partial pressure of 0.25 kPa and with a residence time of 322 s. At a *constant* oxygen partial pressure of 2 kPa, the maximum yield of butadiene was found to be 0.359 (45% of the theoretical maximum yield) with an associated residence time of 58 s.

It is apparent that unlike Case 1, the synthesis of butenes, the maximum yield of butadiene as illustrated in Fig. 10 is extremely sensitive to low oxygen partial pressures.

In Fig. 10 we show the control policy for the partial pressure of oxygen as a function of the yield of butadiene. Fig. 10, in effect, says that the initial partial pressure to the reactor configuration should be approximately 12 kPa and its partial pressure in the tubes should be controlled according to this profile until the yield of butadiene has reached 0.8 carbon mass fraction.

Fig. 11 shows that after a residence time of approximately 1000 s, the oxygen partial pressure has been reduced to 0.07 kPa, i.e. effectively depleted, with a consequential cessation in the further yield of butadiene.

It is clear from Fig. 11 that after approximately 300 s, the oxygen added is only sufficient to keep its partial pressure in the tubes at a very low value and in effect only that which is required to compensate for the oxygen depleted during the oxidation process.

It is concluded that a maximum butadiene yield of 0.8 carbon mass fraction can be obtained from a DSR where the addition of oxygen is rigorously controlled. The total residence time for this

Table 1
Maximum selectivity of *n*-butane to butadiene, residence time and butane concentration for values of oxygen partial pressure.

Oxygen partial pressure (kPa)	Maximum selectivity	Residence time (s)	Butane concentration, carbon mass fraction
85	0.29	34	0.68
2	0.52	34	0.41
1	0.60	66	0.30
0.5	0.67	130	0.20
0.25	0.71	254	0.12
0.1	0.75	613	0.06
0.05	0.77	1 198	0.03

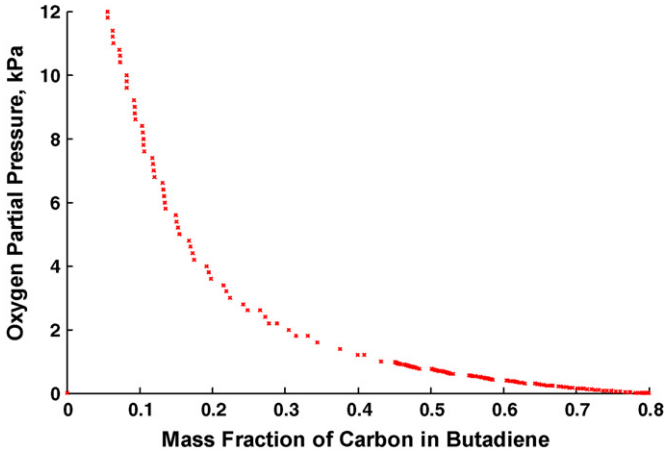

Fig. 10. RCC operational control policy for the maximum yield of butadiene from the ODH of *n*-butane.

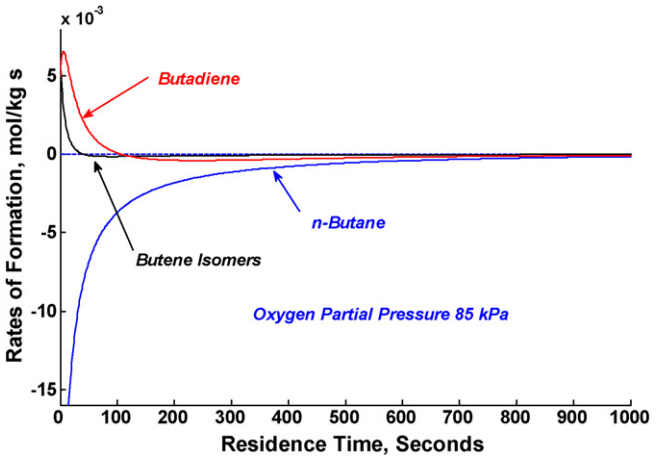

Fig. 12. Rates of formation of butane, butenes, butadiene at a constant oxygen partial pressure of 85 kPa.

yield, according to the RCC algorithm, is 15 000 s. However, according to the RCC algorithm, at a residence time of 1000 s, the yield of butadiene is 0.745 carbon mass fraction, 93% of the theoretical maximum. With a residence time of 332 s, the butadiene yield is 0.665 carbon mass fraction, 83% of the theoretical maximum. If the reaction were ended after 32 s, by which time the oxygen partial pressure had been reduced to 2 kPa, the yield of butadiene would be 0.3 carbon mass fraction of 37% of the theoretical maximum amount.

In Figs. 12 and 13, we show the rates of formation of butane, butene (all three isomers) and butadiene at constant oxygen partial pressure values of 85 kPa and 0.25 kPa.

Scrutiny of Fig. 12 shows that the rates of formation of the three isomers of butene at a constant oxygen partial pressure of 85 kPa initially decline and become negative after a residence time of approximately 40 s. The three isomeric rates of formation are so close together that they cannot be identified separately in Fig. 12 (and in Fig. 13). After this milestone all the butenes resulting from the ODH of butane are oxidised to butadiene, carbon monoxide, carbon dioxide and water at a rate greater than their formation from the oxidation of *n*-butane. In the case of butadiene, initially there is a growth pattern and a peak is attained after a residence time of approximately 5 s. The rate of formation becomes negative after 110 s as the butadiene is oxidised to carbon monoxide, carbon dioxide and water. At an oxygen partial pressure of 85 kPa, the reaction effectively has ceased after a residence time of 1000 s as all the hydrocarbons have been deep oxidised to carbon monoxide, carbon dioxide and water. All the butane has been oxidised after approximately 500 s.

Fig. 13 shows a similar pattern to Fig. 12. At a constant oxygen partial pressure of 0.25 kPa, the rates of formation of the butene isomers become negative after a residence time of 60 s as a consequence of oxidation to butadiene, carbon monoxide, carbon dioxide and water. The initial rate of formation of butadiene reaches a maximum after approximately 90 s and becomes negative after 320 s. Thereafter, the rate of formation of butadiene essentially stays constant at a negative value of 0.002 mol/kg s until 1250 s when effectively it is completely oxidised to carbon monoxide, carbon dioxide and water. The chemical reaction effectively has ceased after 1250 s. All the butane has been oxidised after approximately 500 s.

In Fig. 4, we showed that the ratios of the yields of 1-butene, cis-2-butene to trans-2-butene were constant over the spectrum of oxygen partial pressures from 85 kPa to 0.05 kPa. In Fig. 14 we show that a similar constancy is applicable to the generation of carbon monoxide and carbon dioxide.

In Fig. 14 the mean of the ratios of the moles of carbon dioxide to carbon monoxide at each value of residence time for each value of constant oxygen partial pressure.

The data plotted in Fig. 14 represent the mean values of the CO_2:CO ratio at each oxygen partial pressure over the full gamut of residence time. Superimposed upon Fig. 14 are the minimum and

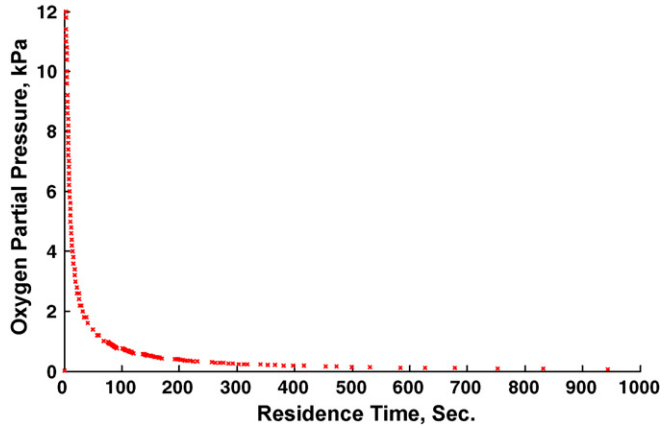

Fig. 11. RCC oxygen control policy as a function of residence time for the maximum yield of butadiene from the ODH of *n*-butane.

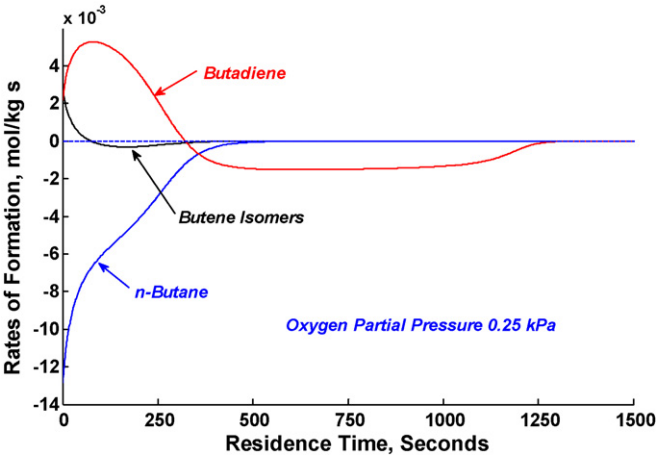

Fig. 13. Rates of formation of butane, butenes and butadiene at a constant oxygen partial pressure of 0.25 kPa.

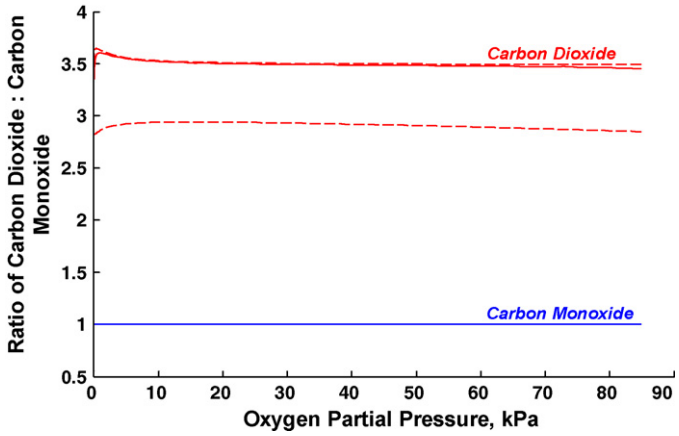

Fig. 14. Molar ratio of yields of carbon dioxide relative to carbon monoxide as function of constant oxygen partial pressure.

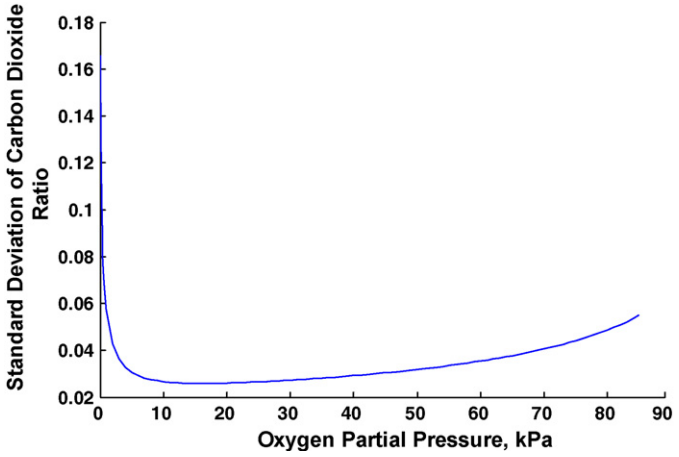

Fig. 15. Standard deviation of the molar ratio of carbon dioxide to carbon monoxide.

maximum values of the carbon dioxide ratio at each oxygen partial pressure. The minimum and maxima values are shown as broken lines. The fact that the mean values are almost coincident with the maximum values despite significantly lower minimum values is a reflection of the consistency of the data. The ratio of formation of carbon dioxide to carbon monoxide over the spectrum of oxygen partial pressures is 3.5 with a slight increase from 20 kPa to 3.6 at 1 kPa and thereafter declining to 3.4 at 0.05 kPa.

As an adjunct to Fig. 14, Fig. 15 shows the standard deviation of the carbon dioxide ratio around its mean value for each oxygen partial pressure.

Figs. 14 and 15 show that over the range of oxygen partial pressures from 85 kPa to 20 kPa, the mean value of the ratio of formation of carbon dioxide to carbon monoxide is 3.5 with a declining standard deviation from 0.055 to 0.026. Below 20 kPa, the ratio increases to 3.6 (standard deviation of 0.06) at 1 kPa and reducing to 3.4 at 0.05 kPa with a standard deviation of 0.166. The minimum standard deviation of the carbon dioxide ratio occurs at an oxygen partial pressure of 16 kPa.

Finally, we wish to comment upon the priority of the alternative paths for the synthesis of butadiene. Referring to Fig. 1, butadiene can be produced either by the direct oxidative dehydrogenation of *n*-butane or via the production of butenes and their subsequent ODH to butadiene. The question is posed as to which of the two reaction paths predominates?

The rate expressions for the ODH of *n*-butane are shown in Table 2. For the production of the butene isomers and butadiene, all these rate expressions are a function of the partial pressure of *n*-butane and of the selective oxidation catalyst sites, θ_0 (Appendix A). When we compare the ratio of the rate expressions for the two reaction paths, the relevant oxygen partial pressures and the oxidation catalyst site expressions cancel each other and we are left with the ratio of the respective rate constants, k_i. The ratio of $(k_1 + k_2 + k_3)$ to k_4 is 4.4 and is independent of the reactor's operating conditions. This means that for every mole of *n*-butane that is directly synthesised to butadiene, 4.4 moles are oxidised to butenes and subsequently to butadiene.

4. Validity of kinetic data

The main thrust of this simulation study was to use the Recursive Convex Control (RCC) algorithm to determine the attainable regions, maximum yields and the optimal reactor configuration for the synthesis of butenes and butadiene from the ODH of *n*-butane. Another reason for using the RCC algorithm was to establish the most favourable reactor operating conditions commensurate with reasonable residence times. What did emerge from his study was the utilisation of low oxygen partial pressures to achieve these ends.

Several authors have expressed opinions, either directly or indirectly, on the validity of kinetic data when applied at low partial pressures of oxygen. Dixon [19] commented that for a reactor, typically of a shell-and-tube configuration, where a reactant is added to the stream of reactants and products the apparently favourable kinetics quoted in the literature might well be unfavourable at the lower partial pressures of the added reactant that seem necessary for the maximisation of the desired product.

The experiments conducted by Téllez et al. [8] on a V/MgO catalyst seemingly spanned a range of oxygen partial pressures from 2 to 10 kPa. Later papers by Téllez et al. [9,20] quoted molar ratios for oxygen to *n*-butane of 0.5–6 and furthermore pointed out that oxygen-rich and oxygen-lean conditions can change the nature of the catalyst significantly. Assabumrungrat et al. [18] in their research paper used an air to *n*-butane ratio of 8 in the reactant feed as the standard condition but their experiments were carried out over a range of air ratios between 1 and 15. This ratio range corresponds to oxygen to *n*-butane molar ratios of 0.2–3. These limits, in turn, correspond to initial oxygen partial pressures of 18–76 kPa. Cortés et al. [21] studied the kinetics of a modified V/MgO catalyst in a fluidised-bed reactor under anaerobic conditions and claimed an improvement in the selectivity of butane to butenes and butadiene.

We have found that the yield of butenes seemingly is unaffected by low oxygen partial pressures since yields close to the theoretical maximum are feasible at an oxygen partial pressure of 2 kPa, this being the lower limit used by Téllez et al. (Fig. 5). This is not the case in the synthesis of butadiene where the yield is highly sensitive to the oxygen partial pressure (Fig. 10).

Whereas we are not concerned unduly with the higher values of oxygen partial pressure, the kinetic data used in this study at low oxygen partial pressures require corroboration or, if found wanting, replaced with data that, like Caesar's wife, are above suspicion.

This simulation study, *inter alia*, has emphasised the importance low oxygen partial pressures and, *a fortiori*, the need for reliable kinetic data under these conditions. Consequently, the validity of our kinetic data at low oxygen partial pressures must be taken as being unproven and of qualified applicability.

5. Conclusions

The attainable region analysis of the ODH of *n*-butane and 1-butene has been undertaken using the Recursive Convex Control

(RCC) algorithm. Whereas earlier simplistic approaches depended upon a starting premise of a specific reactor configuration, the RCC algorithm does not and the optimal reactor configuration for attainment of the AR^C emerges from the algorithm as an output.

The simulation study shows that for the ODH of *n*-butane to butenes and butadiene a differential side-stream catalytic membrane reactor with predefined control patterns for the addition of oxygen can result in yields of hydrocarbon product close to the theoretical maxima. Yields of butenes, in contrast to butadiene, are relatively unaffected by low values of oxygen partial pressure.

Ratios of formation of butene isomers and carbon dioxide to carbon monoxide were shown to be constant over a wide range of oxygen partial pressures.

The synthesis of butenes from the ODH of *n*-butane proceeds faster than the direct synthesis of butadiene by a factor of 4.4.

The validity of the kinetic data at low values of oxygen partial pressure remains unproven and requires corroboration.

Appendix A.

Téllez et al. [8,9] identified the independent balanced chemical reactions involved in the ODH (Fig. 1) of butane and their associated rate expressions as:

In Table 2, θ_0 and λ_0 refer to the oxidation of catalyst sites and are defined as:

Selective oxidation catalyst sites

$$\theta_0 = \frac{2k_{12}p_{\text{oxygen}}}{2k_{12}p_{\text{oxygen}} + (k_1 + k_2 + k_3 + 2k_4)p_{\text{butane}} + k_7 p_{\text{butenes}}}$$

Non-selective oxidation catalyst sites

$$\lambda_0 = \frac{2k_{13}p_{\text{oxygen}}}{2k_{13}p_{\text{oxygen}} + (9k_5 + 3k_6)p_{\text{butane}} + (8k_8 + 2k_9)p_{\text{butenes}} + (7k_{10} + 11k_{11})p_{\text{butadiene}}}$$

X and Z refer to the reduced active sites of the catalyst.

X_0 and Z_0 refer to the oxidised active sites of the catalyst.

p_i is the partial pressure of the subscripted species, *i*, atm.

The rate expressions presented by Téllez et al. [8,9] indicate a dependency upon the partial pressures of butane, butene and butadiene and the selective (θ_0) and non-selective (λ_0) oxidation catalyst sites respectively. The latter two, in turn, are functions of the partial pressure of oxygen and of the partial pressures of butane, butene and butadiene.

Because the partial pressure of oxygen influences the selective and non-selective oxidation catalyst sites which in turn affects the rate expressions it was adopted as the primary independent control variable.

The kinetic data for the system *n*-butane:butenes:butadiene used in this study were taken from Téllez et al. [8,9] and from Assabumrungrat et al. [18] and are shown in Table 3.

Table 2
Chemical reactions and rate expressions for the oxidative dehydrogenation of *n*-butane to butene and butadiene.

Reaction		Rate expression
Oxidation of *n*-butane		
$C_4H_{10} + 1/2O_2 \rightarrow$ 1-$C_4H_8 + H_2O$	(1)	$r_1 = k_1 P_{C_4H_{10}} \theta_0$
$C_4H_{10} + 1/2O_2 \rightarrow$ Trans-2-$C_4H_8 + H_2O$	(2)	$r_2 = k_2 P_{C_4H_{10}} \theta_0$
$C_4H_{10} + 1/2O_2 \rightarrow$ Cis-2-$C_4H_8 + H_2O$	(3)	$r_3 = k_3 P_{C_4H_{10}} \theta_0$
$C_4H_{10} + O_2 \rightarrow C_4H_6 + 2H_2O$	(4)	$r_4 = k_4 P_{C_4H_{10}} \theta_0$
$C_4H_{10} + 9/2O_2 \rightarrow 4CO + 5H_2O$	(5)	$r_5 = k_5 P_{C_4H_{10}} \lambda_0$
$C_4H_{10} + 13/2O_2 \rightarrow 4CO_2 + 5H_2O$	(6)	$r_6 = k_6 P_{C_4H_{10}} \lambda_0$
Oxidation of 1-butene		
1-$C_4H_8 + 1/2O_2 \rightarrow C_4H_6 + H_2O$	(7)	$r_7 = k_7 P_{C_4H_8} \theta_0$
1-$C_4H_8 + 4O_2 \rightarrow 4CO + 4H_2O$	(8)	$r_8 = k_8 P_{C_4H_8} \lambda_0$
1-$C_4H_8 + 6O_2 \rightarrow 4CO_2 + 4H_2O$	(9)	$r_9 = k_9 P_{C_4H_8} \lambda_0$
Oxidation of butadiene		
$C_4H_6 + 7/2O_2 \rightarrow 4CO + 3H_2O$	(10)	$r_{10} = k_{10} P_{C_4H_6} \lambda_0$
$C_4H_6 + 11/2O_2 \rightarrow 4CO_2 + 3H_2O$	(11)	$r_{11} = k_{11} P_{C_4H_6} \lambda_0$
Oxidation and reduction of catalyst sites		
$O_2 + 2X \rightarrow 2X_0$	(12)	$r_{12} = k_{12} P_{O_2} (1 - \theta_0)$
$O_2 + 2Z \rightarrow 2Z_0$	(13)	$r_{13} = k_{13} P_{O_2} (1 - \lambda_0)$

The rate constant, $k_i = k_{io} \exp(-(E_a i/R)(1/T - 1/T_0))$, where $T_0 = 773$ K.

The equations for rates of formation, r_1 to r_9, of the several species are:

n-Butane

$$r_1 = -((k_1 + k_2 + k_3 + k_4)\theta_0 + (k_5 + k_6)\lambda_0)p_{\text{butane}}$$

Oxygen

$$a_1 = ((k_1 + k_2 + k_3 + k_4)\theta_0 + (9k_5 + 13k_6)\lambda_0)0.5p_{\text{butane}}$$
$$a_2 = (k_7\theta_0 + 8k_8\lambda_0)0.5p_{\text{butenes}} + 12 \times 0.5k_9 p_{\text{butenes}}\lambda_0$$
$$a_3 = (7k_{10} + 11k_{11})0.5\lambda_0 p_{\text{butadiene}}$$
$$a_4 = (k_{12}(1 - \theta_0) + k_{13}(1 - \lambda_0))0.5p_{\text{oxygen}}$$

$$r_2 = -(a_1 + a_2 + a_3 + a_4)$$

1-Butene

$$r_3 = (k_1 p_{\text{butane}} - k_7 p_{\text{1-butene}})\theta_0 - (k_8 + k_9)p_{\text{1-butene}}\lambda_0$$

Trans-2-butene

$$r_4 = (k_2 p_{\text{butane}} - k_7 p_{\text{trans-2-butene}})\theta_0 - (k_8 + k_9)p_{\text{trans-2-butene}}\lambda_0$$

Table 3
Rate constants and activity coefficients from Téllez et al. [8,9] and Assabumrungrat et al. [18].

Reaction	Rate constant, k_{io} (mol/kg s)	Activity coefficient, E_{ai} (kJ/mol)
$C_4H_{10} + 1/2O_2 \rightarrow$ 1-$C_4H_8 + H_2O$	62.33×10^{-3}	144.9
$C_4H_{10} + 1/2O_2 \rightarrow$ Trans-2-$C_4H_8 + H_2O$	32.83×10^{-3}	142.7
$C_4H_{10} + 1/2O_2 \rightarrow$ Cis-2-$C_4H_8 + H_2O$	39.67×10^{-3}	139.1
$C_4H_{10} + O_2 \rightarrow C_4H_6 + 2H_2O$	30.83×10^{-3}	148.5
$C_4H_{10} + 9/2O_2 \rightarrow 4CO + 5H_2O$	9.17×10^{-3}	175.5
$C_4H_{10} + 13/2O_2 \rightarrow 4CO_2 + 5H_2O$	25.83×10^{-3}	138.4
$C_4H_8 + 1/2O_2 \rightarrow C_4H_6 + H_2O$	685.0×10^{-3}	164.7
$C_4H_8 + 4O_2 \rightarrow 4CO + 4H_2O$	32.33×10^{-3}	146.2
$C_4H_8 + 6O_2 \rightarrow 4CO_2 + 4H_2O$	115.67×10^{-3}	107.2
$C_4H_6 + 7/2O_2 \rightarrow 4CO + 3H_2O$	118.17×10^{-3}	146.6
$C_4H_6 + 11/2O_2 \rightarrow 4CO_2 + 3H_2O$	435×10^{-3}	102.0
$O_2 + 2X \rightarrow 2X_0$	2995×10^{-3}	114.5
$O_2 + 2Z \rightarrow 2Z_0$	3255×10^{-3}	5.5

Cis-2-butene

$$r_5 = (k_3 p_{\text{butane}} - k_7 p_{\text{cis-2-butene}})\theta_0 - (k_8 + k_9) p_{\text{cis-2-butene}} \lambda_0$$

Butadiene

$$r_6 = (k_4 p_{\text{butane}} + k_7 p_{\text{butenes}})\theta_0 - (k_{10} + k_{11}) p_{\text{butadiene}} \lambda_0$$

Carbon monoxide

$$r_7 = 4(k_5 p_{\text{butane}} \lambda_0 + k_8 p_{\text{butenes}} \lambda_0 + k_{10} p_{\text{butadiene}} \lambda_0)$$

Carbon dioxide

$$r_8 = 4(k_6 p_{\text{butane}} \lambda_0 + k_9 p_{\text{butenes}} \lambda_0 + k_{11} p_{\text{butadiene}} \lambda_0)$$

Water

$$r_9 = (k_1 + k_2 + k_3 + 2k_4) p_{\text{butane}} \theta_0 + 5(k_5 + k_6) p_{\text{butane}} \lambda_0 + (k_7 p_{\text{butenes}} \theta_0 + 4(k_8 + k_9) p_{\text{butenes}} \lambda_0 + 3(k_{10} + k_{11}) p_{\text{butadiene}} \lambda_0)$$

In these equations, p refers to the partial pressure of the subscripted hydrocarbon and the rate constants k_1 to k_{13} are those shown in Table 3. θ_0 and λ_0, the selective and non-selective oxidation catalysts sites, are as defined earlier.

References

[1] M. Feinberg, D. Hildebrandt, Chemical Engineering Science 52 (10) (1997) 1637–1665.
[2] D. Glasser, D. Hildebrandt, C.M. Crowe, American Chemical Society (1987) 1803–1810.
[3] D. Glasser, D. Hildebrandt, C.M. Crowe, Industrial and Engineering Chemistry Research 26 (1987) 1803–1810.
[4] M. Feinberg, Chemical Engineering Science 55 (2000) 2455–2479.
[5] M. Feinberg, Chemical Engineering Science 55 (2000) 3553–3565.
[6] T.G. Seodigeng, PhD Thesis, University of the Witwatersrand, Johannesburg, South Africa, 2006.
[7] T.G. Seodigeng, B. Hausberger, D. Hildebrandt, D. Glasser, Computers and Chemical Engineering 33 (1) (2009) 309–320.
[8] C. Téllez, M. Menéndez, J. Santamaría, Journal of Catalysis 183 (1999) 210–221.
[9] C. Téllez, M. Menéndez, J. Santamaría, Chemical Engineering Science 54 (1999) 2917–2925.
[10] D. Milne, D. Glasser, D. Hildebrandt, B. Hausberger, Industrial and. Engineering Chemistry Research 43 (2004) 1827–1831 (with corrections subsequently published in Industrial and Engineering Chemistry Research 43 (2004), 7208).
[11] D. Milne, D. Glasser, D. Hildebrandt, B. Hausberger, Industrial and Engineering Chemistry Research 45 (2006) 2661–2671.
[12] D. Hildebrandt, D. Glasser, C. Crowe, Industrial and Engineering Chemistry Research 29 (49) (1990) 49–58.
[13] W. Nicol, M. Hernier, D. Hildebrandt, D. Glasser, Chemical Engineering Science 56 (2001) 173–191.
[14] S. Godorr, D. Hildebrandt, D. Glasser, C. McGregor, Industrial and Engineering Chemistry Research 38 (3) (1999) 639–651.
[15] D. Milne, T. Seodigeng, D. Glasser, D. Hildebrandt, B. Hausberger, Industrial and Engineering Chemistry Research 48 (11) (2009) 5211–5222.
[16] T.K. Abraham, M. Feinberg, Industrial and Engineering Chemistry Research 43 (2004) 449–457.
[17] D. Milne, D. Glasser, D. Hildebrandt, B. Hausberger, Chemical Engineering Progress 102 (3) (2006) 46–51 (with corrections subsequently published in Chemical Engineering Progress 102(7) (2006) 6).
[18] S. Assabumrungrat, T. Rienchalanusarn, P. Praserthdam, S. Goto, Chemical Engineering Journal 85 (2002) 69–79.
[19] A.G. Dixon, Catalysis, vol. 14, The Royal Society of Chemistry, 1999, pp. 40–92.
[20] C. Téllez, M. Abon, J.A. Dalmon, C. Mirodatos, J. Santamaría, Journal of Catalysis, Chemical Engineering Science 195 (2000) 113–124.
[21] I. Cortés, O. Rubio, J. Herguido, M. Menéndez, Catalysis Today 91 (2004) 281–284.